Few-Shot Learning as Domain Adaptation: Algorithm and Analysis

Jiechao Guan [1] **Zhiwu Lu** [1] **Tao Xiang** [2] **Ji-Rong Wen** [1]

Abstract

To recognize the unseen classes with only few samples, few-shot learning (FSL) uses prior knowledge learned from the seen classes. A major challenge for FSL is that the distribution of the unseen classes is different from that of those seen, resulting in poor generalization even when a model is meta-trained on the seen classes. This class-difference-caused distribution shift can be considered as a special case of domain shift. In this paper, for the first time, we propose a domain adaptation prototypical network with attention (DAPNA) to explicitly tackle such a domain shift problem in a meta-learning framework. Specifically, armed with a set transformer based attention module, we construct each episode with two sub-episodes without class overlap on the seen classes to simulate the domain shift between the seen and unseen classes. To align the feature distributions of the two sub-episodes with limited training samples, a feature transfer network is employed together with a margin disparity discrepancy (MDD) loss. Importantly, theoretical analysis is provided to give the learning bound of our DAPNA. Extensive experiments show that our DAPNA outperforms the state-of-the-art FSL alternatives, often by significant margins.

1. Introduction

Learning with only few samples to recognize an unseen class is the hallmark of human intelligence. However, such an ability is still beyond existing artificial intelligence systems. Despite the recent great success of various deep learning techniques (He et al., 2016; McCann et al., 2017), the requirement of a large number of training samples per class

still hinders their applications in many real-life scenarios. To overcome this challenge, few-shot learning (FSL) (Li et al., 2006), which uses prior knowledge learned from the seen classes and several shots from the unseen classes, becomes topical in the past few years.

FSL (Snell et al., 2017; Sun et al., 2019) is often formulated as a form of transfer learning (Pan & Yang, 2010) from the seen/source classes to the unseen/target ones. Existing FSL studies include meta-learning based methods (Finn et al., 2017; 2018; Rusu et al., 2019), metric-learning based methods (Vinyals et al., 2016; Snell et al., 2017; Ye et al., 2018), and classifier-learning based methods (Qiao et al., 2018; Lee et al., 2019b; Chen et al., 2019), which instantiate the transferable knowledge as a network initialization condition, a metric space, and a predicted classifier, respectively. However, there is an additional challenge which has been neglected so far, that is, the distribution of the unseen classes is different from that of those seen during training. Such a distribution difference/shift is caused by class label difference. This differs from the problem domain difference as studied in the classic domain adaptation (DA) problems (Ben-David et al., 2010; Muandet et al., 2013; Zhang et al., 2019b), where the source and target datasets contain the same classes but come from different domains (e.g., train a cat classifier on paintings and recognize cats in photos). However, it has the same effect of leading to poor generalization of the model trained on the source data, and thus can be considered as a special case of domain shift.

In this paper, for the first time, we propose to tackle this class-difference-caused domain shift problem (Chen et al., 2019) jointly with FSL in a unified meta-learning framework. Note that the domain shift problem has not been explicitly addressed in the evaluation paper (Chen et al., 2019). Even though both DA and FSL have been studied intensively and a variety of methods exist to address each problem independently, addressing both problems jointly in a unified meta-learning framework is non-trivial. The primary challenge is to estimate and align the data distribution with few training samples. To this end, a novel meta-learning model termed domain adaptation prototypical network with attention (DAPNA) is proposed, which seamlessly combines FSL and DA in a single framework.

Concretely, we first introduce a set transformer (Lee et al.,

[1]Beijing Key Laboratory of Big Data Management and Analysis Methods, Gaoling School of Artificial Intelligence, Renmin University of China, Beijing 100872, China. [2]Department of Electrical and Electronic Engineering, University of Surrey, Guildford, Surrey GU2 7XH, United Kingdom. Correspondence to: Zhiwu Lu <luzhiwu@ruc.edu.cn>.

2019a) based instance attention module into the Prototypical Network (ProtoNet) (Snell et al., 2017), so that the few training samples of each class is better combined to represent the class compared to the simple average used in ProtoNet. Crucially, in order to meta-learn a model that is intrinsically robust against the domain shift caused by class difference, each meta-training episode now contains two sub-episodes running in parallel; each sub-episode contains a set of different seen classes. The model is then forced to align the distributions of the samples in the two sub-episodes in a shared feature embedding space. Note that each sub-episode still consists of very limited number of samples, challenging existing DA methods. To overcome this problem, we adopt a feature transfer network with an encoder-decoder architecture to assist in domain alignment. Further, a margin disparity discrepancy (MDD) loss (Zhang et al., 2019b) is employed to reduce the domain gap between the two sub-episodes. Our comparative results (Table 1) and ablative results (Figure 2) demonstrate the significant advantages of introducing meta-DA for meta-learning based FSL. Importantly, we also provide a theoretical analysis to give the learning bound of our DAPNA model.

Our contributions are: (1) For the first time, we propose that the conventional FSL problem must be solved together with the DA problem, and a novel DAPNA model is developed by introducing meta-DA into ProtoNet. (2) We provide the first rigorous learning bound of meta-learning based FSL in the area of FSL. (3) Our DAPNA model achieves new state-of-the-art performance on three standard FSL and one cross-domain FSL benchmark datasets.

2. Related Work

Few-Shot Learning Most FSL methods are based on meta learning consisting of two stages: meta-training and meta-testing (Chen et al., 2019). During the meta-training stage, a feature extractor and a classifier are learned from a large set of source/seen classes. During meta-testing, a set of unseen target classes with few-shots in each class are used together with the meta-trained model to recognize unseen classes. Specifically, existing FSL models can be categorized into the following four groups: (1) *recurrent-neural-network* based approaches (Mishra et al., 2018; Munkhdalai & Yu, 2017; Munkhdalai et al., 2018) are always equipped with an external or internal memory storage to store the transferable knowledge. (2) *initialization* based methods (Finn et al., 2017; Li et al., 2017; Finn et al., 2018; Lee & Choi, 2018) aim to learn a great initial parameter condition of base feature extractor, and then fine-tune the network to the unseen classes using just several examples within a few gradient steps. (3) *classifier-learning* based models (Ye et al., 2018; Qiao et al., 2018; Chen et al., 2019; Lee et al., 2019b; Ren et al., 2019) train a feature extractor in meta-training and

fix it during meta-testing whilst learning a new classifier (e.g., linear softmax classifier) for the unseen classes. (4) *metric-learning* based variants (Vinyals et al., 2016; Snell et al., 2017; Ye et al., 2018; Zhang et al., 2019a) utilize nearest neighbour search strategy to find the most possible class label for the unseen samples. Since the nearest neighbour classifier (e.g. based on Euclidean distance) is a non-parametric model, this kind of models only need to run a forward pass during the meta-testing stage without the need to update the feature extractor parameters. Besides the above four main groups, there are other FSL methods such as those utilizing semantic information (Li et al., 2019; Xing et al., 2019) or using the feature-wise transformation for cross-domain FSL (Tseng et al., 2020). Our DAPNA belongs to the fourth group. However, differing from any existing FSL model, it *explicitly* addresses the domain shift problem caused by the difference between the seen and unseen classes in a two-sub-episode meta-training framework.

Domain Adaptation (Pan & Yang, 2010) aims to generalize the learned model to different domains or different distributions. (Mansour et al., 2009; Ben-David et al., 2010) provide theoretical foundations and rigorous learning bounds of unsupervised DA under the Probably Approximately Correct (PAC) framework (Valiant, 1984). From then on, a number of DA algorithms minimizing the distribution discrepancy or learning bounds are proposed, either based on adversarial learning (Goodfellow et al., 2014; Ganin et al., 2016; Long et al., 2018) or statistic matching (Long et al., 2015). Note that in all existing DA works, the source and target domains are assumed to contain the same set of classes. In this work, we first identify the fact that the domain shift issue (Gretton et al., 2009) also exists in the conventional FSL problem, even if the seen and unseen classes are from the same problem domain. This class-difference-caused domain shift is *unique and hard to solve* due to the few available training samples. In this work, we construct each episode with two sub-episodes without class overlap to serve as the source and target domains for DA during meta-training. Our extensive experiments show that introducing such meta-DA significantly improves the cross-domain transferability of the learned model. Note that FSL and DA have been combined in (Motiian et al., 2017). However, the problem setting in (Motiian et al., 2017) is very different – the target domain has the same set of classes as the source domain but has only few samples for DA.

3. Methodology

3.1. Problem Definition

Under the FSL setting, we are given a large sample set $\mathcal{D}_s$ from a set of source classes $\mathcal{C}_s$, a few-shot sample set $\mathcal{D}_t$ from a set of target classes $\mathcal{C}_t$, and a test set $\mathcal{T}$ from $\mathcal{C}_t$, where $\mathcal{C}_s \bigcap \mathcal{C}_t = \emptyset$. The focus is thus on training a

classification model with $\mathcal{D}_s$ that can generalize well to $\mathcal{T}$. Note that the few-shot sample set $\mathcal{D}_t$ from $\mathcal{C}_t$ can also be used for model training. However, we follow the FSL setting that does not require fine-tuning to the unseen classes and thus ignore $\mathcal{D}_t$ in the training phase. This enables fast model deployment to the unseen classes.

We then define the episodic training strategy widely used by existing meta-learning based FSL models (Snell et al., 2017; Sung et al., 2018; Kim et al., 2019). Concretely, a meta-learning based FSL model is trained over n-way k-shot classification tasks randomly sampled from $\mathcal{D}_s$, and each n-way k-shot task is defined over an episode $D = \{S, Q\}$, where S is the support set containing n classes and k samples per class, and Q is the query set with the same n classes. The episode $D = \{S, Q\}$ can be constructed as follows: we first select a small set of source class $\mathcal{C} = \{\mathcal{C}_i \mid i = 1, ..., n\}$ from $\mathcal{C}_s$, and then generate S and Q by randomly sampling k support samples and q query samples from each class in $\mathcal{C}$, respectively. Formally, we have $S = \{(x_i, y_i) \mid y_i \in \mathcal{C}, i = 1, ..., n \times k\}$ and $Q = \{(x_i, y_i) \mid y_i \in \mathcal{C}, i = 1, ..., n \times q\}$, where $S \bigcap Q = \emptyset$ and y_i denotes the class label of x_i. The model is then trained by minimizing the loss function between its predicted labels and the ground-truth labels over the query set Q in each episode.

3.2. Few-Shot Learning Module

3.2.1. PROTOTYPICAL NETWORKS

Since Prototypical Network (ProtoNet) (Snell et al., 2017) is used as our baseline model, it is briefly introduced here. ProtoNet learns a *prototype* of each class in the support set S and classifies each sample in the query set Q based on its distances to different prototypes. We use ϕ to define the convolutional neural network (CNN) embedding function which maps a sample x_i to a visual feature vector $\phi(x_i)$. Each prototype p_c is the mean vector of the embedded support samples belonging to the class c:

$$p_c = \frac{1}{|S_c|} \sum_{(x_i, y_i) \in S_c} \phi(x_i) \qquad (1)$$

where $S_c \in S$ denotes the set of support samples that belong to the class c. ProtoNet thus produces the class distributions of a query sample x_i based on the softmax output w.r.t. the distance between $\phi(x_i)$ and the class prototype p_c:

$$p(y_i = c | x_i) = \frac{\exp(-d(\phi(x_i), p_c))}{\sum_{c'} \exp(-d(\phi(x_i), p_{c'}))} \qquad (2)$$

where $d(\cdot, \cdot)$ denotes the Euclidean distance metric in the visual feature space. The loss function for ProtoNet is defined based on the negative log-probability of a query sample x_i having the ground-truth class label c:

$$L_p = - \sum_{x_i \in Q} \log p(y_i = c | x_i) \qquad (3)$$

3.2.2. ATTENTION MECHANISM

In ProtoNet, a class is represented as the mean of the few training samples. However, representing a class prototype simply as sample mean may not be the optimal strategy, especially when only few samples are available, e.g., a single outlying sample can introduce large bias into the prototype. We thus propose to learn the best way to representing a set of training samples using a single class prototype by introducing a set transformer based attention mechanism (Lee et al., 2019a). Concretely, we construct a triplet (query, key, value): the query point is matched against a list of keys where each key has a value; the similarities between the query point and the keys are computed; the final value is represented as the sum of all the values weighted by the computed similarities. Formally, we use $\mathcal{U}$ to denote the set of query points with $\mathcal{K}$ for keys and $\mathcal{V}$ for values:

$$
\begin{aligned}
U &= W_U^T [\phi(x_i), \forall x_i \in \mathcal{U}] \in \mathbb{R}^{d \times |\mathcal{U}|} \\
K &= W_K^T [\phi(x_i), \forall x_i \in \mathcal{K}] \in \mathbb{R}^{d \times |\mathcal{K}|} \qquad (4) \\
V &= W_V^T [\phi(x_i), \forall x_i \in \mathcal{V}] \in \mathbb{R}^{d \times |\mathcal{V}|}
\end{aligned}
$$

where d is the dimension of the elements in U, K, V. The similarity between a query point $x_i \in \mathcal{U}$ and a key in $\mathcal{K}$ is then computed as "attention": $\alpha_{ij} \propto \exp \phi(x_i)^T W_U W_K^T \phi(x_j) / \sqrt{d}$, where $x_i \in \mathcal{U}$ and $x_j \in \mathcal{K}$. These attentions are used as weights to compute the final embeddings for the query point x_i:

$$\tilde{\phi}(x_i) = \phi(x_i) + \sum_{x_l \in V} \alpha_{il} W_V^T \phi(x_l) \qquad (5)$$

After converting the instance representation $\phi(x_i)$ into the new one $\tilde{\phi}(x_i)$, we still use Eqs. (1)-(2) to compute the prototype for each class, just with $\tilde{\phi}(x_i)$ as input. The obtained model is called as ProtoNet with Attention (PNA). For simplicity, we set the triplet elements uniformly as the support set in one episode: $\mathcal{U} = \mathcal{K} = \mathcal{V} = S (\in D)$.

3.3. Domain Adaptation Module

Before introducing a domain adaptation (DA) module into our FSL framework, we need to apply transformation on the original features of each training sample to the feature embedding space less sensitive to which domain the sample belongs to. To this end, we introduce a feature transfer network to transform the instance features to be domain confused in the feature embedding space and maintain the instance features discriminative before feature embedding. Specifically, we add an encoder-decoder network (as shown in Figure 1) on the top of the backbone for feature embedding. More details and explanations about the feature embedding layer can be found in the suppl. material.

Furthermore, to simulate the domain shift between the seen and unseen classes, we construct each episode $D = \{S, Q\}$
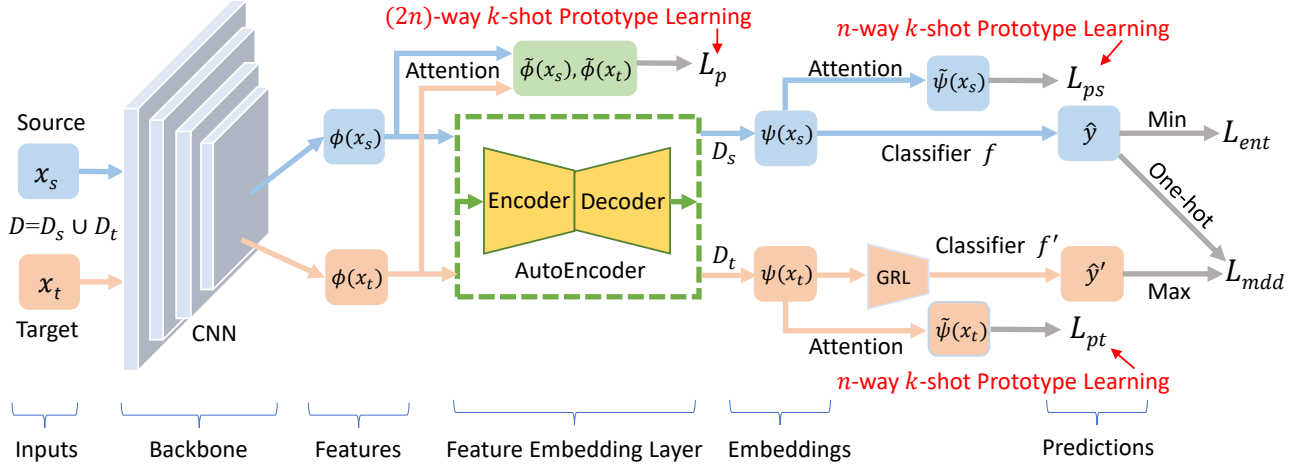
Figure 1. Illustration of our proposed DAPNA model. To simulate the domain shift between the seen and unseen classes, we construct each episode D (e.g. 10-way 5-shot 15-query) with two sub-episodes D_s, D_t (e.g. 5-way 5-shot 15-query) without class overlap, which respectively serve as the source and target domains for meta-DA after the feature embedding layer.

(e.g. 10-way 5-shot 15-query) over the seen classes with two sub-episodes $D_s = \{S_s, Q_s\}$ and $D_t = \{S_t, Q_t\}$ without class overlap: each sub-episode contains the same number of samples (e.g. 5-way 5-shot 15-query) but has a set of different classes. We then compute the PNA losses (see Sec. 3.2) over these two sub-episode as follows:

$$L_{ps} = - \sum_{x_i \in Q_s} \log p(y_i = c | x_i)$$
$$L_{pt} = - \sum_{x_i \in Q_t} \log p(y_i = c | x_i)$$
(6)

where $p(y_i = c | x_i)$ is similar to that in Eq. (2) with the only difference that the embedding function ϕ is changed to ψ, and an attention mechanism is used as in Eq. (5) with only the transformer $\tilde{\phi}$ being replaced by $\tilde{\psi}$. Note that we have $\psi = \phi$ when the feature embedding layer is not used.

With the above episode definition, we can readily introduce DA into meta-training. Concretely, we treat one sub-episode D_s as the source domain, and the other sub-episode D_t as the target domain. We expect to narrow the domain gap between D_s and D_t by meta-DA. This is achieved by backpropagating a DA loss to the backbone network. The advantage lies in that the transferability of the learned model can be improved in the meta-learning framework.

3.3.1. MARGIN LOSS

Taking the notations of (Mohri et al., 2012), we consider multi-class classification with hypothesis space $\mathcal{F}$ of scoring function $f : \mathcal{X} \to \mathcal{Y}, \mathcal{X} = \bigcup_{x_i \in \mathcal{D}_s} x_i, \mathcal{Y} = C_s$. We use $f(x_i, y_i)$ to indicate the component of $f(x_i)$ corresponding to the class label y_i. Then it induces a labeling function space $\mathcal{H}$ containing h_f from $\mathcal{X}$ to $\mathcal{Y}$:

$$h_f : x_i \to \arg\max_{y \in \mathcal{Y}} f(x_i, y)$$
(7)

The expected error rate of a labeling function $h \in \mathcal{H}$ w.r.t. distribution $\widetilde{D}$ (where episode D is drawn from) is given by

$$err_{\widetilde{D}}(h) \triangleq \mathbb{E}_{(x_i, y_i) \sim \widetilde{D}} \mathbb{1}[h(x_i) \neq y_i]$$
(8)

The margin of a hypothesis f at a labeled sample (x_i, y_i) is

$$\rho_f(x_i, y_i) \triangleq \frac{1}{2}(f(x_i, y_i) - \max_{y \neq y_i} f(x_i, y))$$
(9)

The *empirical margin loss* of a hypothesis f is

$$err_D^{(\rho)}(f) \triangleq \frac{1}{|D|} \sum_{i=1}^{|D|} \Phi_\rho \circ \rho_f(x_i, y_i)$$
(10)

where $\circ$ denotes function composition and Φ_ρ is

$$\Phi_\rho(x) \triangleq \begin{cases} 0 & \rho \leq x \\ 1 - x/\rho & 0 \leq x \leq \rho \\ 1 & x \leq 0 \end{cases}$$
(11)

3.3.2. MARGIN DISPARITY DISCREPANCY

For each meta-training step, inspired by (Zhang et al., 2019b), we define an improved discrepancy named margin disparity discrepancy (MDD) to measure the distribution difference between the source and target sub-episodes by restricting the hypothesis space.

Definition 3.1 (Margin Disparity Discrepancy) *The empirical margin disparity discrepancy (MDD) over the source and target sub-episodes is defined as:*

$$d_{f, \mathcal{F}}^{(\rho)}(D_s, D_t) \triangleq \sup_{f' \in \mathcal{F}} (\mathrm{disp}_{D_t}^{(\rho)}(f', f) - \mathrm{disp}_{D_s}^{(\rho)}(f', f))$$
(12)

where D_s and D_t are the source and target sub-episodes respectively, and $\mathrm{disp}_D^{(\rho)}(f', f) \triangleq \mathbb{E}_D \Phi_\rho \circ \rho_{f'}(\cdot, h_f) = \frac{1}{|D|} \sum_{i=1}^{|D|} \Phi_\rho \circ \rho_{f'}(x_i, h_f(x_i))$ is the margin disparity.

Definition 3.2 (Rademacher Complexity) *Let $\mathcal{F}$ be a family of functions mapping from $\mathcal{Z} = \mathcal{X} \times \mathcal{Y}$ to $[a, b]$ and $D = \{z_1, ..., z_m\}$ be a fixed sample set of size m drawn from the distribution $\widetilde{D}$ over $\mathcal{Z}$. The empirical Rademacher Complexity of $\mathcal{F}$ w.r.t. the sample set D is defined as*

$$\widehat{\mathfrak{R}}_D(\mathcal{F}) \triangleq \mathbb{E}_\sigma \sup_{f \in \mathcal{F}} \frac{1}{m} \sum_{i=1}^{m} \sigma_i f(z_i) \quad (13)$$

where σ_i $(i = 1, ..., m)$ are i.i.d. uniform random variables taking values in $\{-1, +1\}$. We further have the following Rademacher Complexity of the distribution $\widetilde{D}$:

$$\mathfrak{R}_{|D|, \widetilde{D}}(\mathcal{F}) \triangleq \mathbb{E}_{D \sim \widetilde{D}} \widehat{\mathfrak{R}}_D(\mathcal{F}) \quad (14)$$

where $|D|$ is the number of elements in D.

As mentioned above, we treat one sub-episode D_s as the source domain and the other D_t as the target one. We thus have the following theorem on the learning bound for any classifier f over the target domain distribution $\widetilde{D}_t$.

Theorem 3.1 (Learning Bound of DA) *For any $\delta > 0$, with probability $1 - 3\delta$, the uniform learning bound for any classifier f over $\widetilde{D}_t$ is:*

$$err_{\widetilde{D}_t}(h_f) \le err_{D_s}^{(\rho)}(f) + d_{f,F}^{(\rho)}(D_s, D_t) + \lambda_1$$
$$+ \frac{2N^2}{\rho} \mathfrak{R}_{|D_s|, \widetilde{D}_s}(\Pi_1 \mathcal{F}) + \frac{N}{\rho} \mathfrak{R}_{|D_s|, \widetilde{D}_s}(\Pi_{\mathcal{H}} \mathcal{F})$$
$$+ \frac{N}{\rho} \mathfrak{R}_{|D_t|, \widetilde{D}_t}(\Pi_{\mathcal{H}} \mathcal{F}) + 2\sqrt{\frac{\log \frac{2}{\delta}}{2|D_s|}} + \sqrt{\frac{\log \frac{2}{\delta}}{2|D_t|}} \quad (15)$$

where λ_1 is a constant independent of f, $\mathfrak{R}_{|D|, \widetilde{D}}(\mathcal{F})$ is the Rademacher Complexity of $\mathcal{F}$ w.r.t. the sample set D drawn from distribution $\widetilde{D}$, $\Pi_{\mathcal{H}}(F) \triangleq \{x \mapsto f(x, h(x)) | h \in \mathcal{H}, f \in \mathcal{F}\}$, $\Pi_1 \mathcal{F} \triangleq \{x \mapsto f(x, y) | y \in \mathcal{Y}, f \in \mathcal{F}\}$, and N is the number of classes in $\mathcal{C}_s$ (i.e. $N = |\mathcal{C}_s|$).

By regarding sub-episodes as domains, the above theorem can be easily proven just as Theorem 3.7 of (Zhang et al., 2019b), which is ignored for compactness. Following most recent DA methods, we select the first two terms of the learning bound for DA (Rademacher complexities are constants w.r.t. f). Our meta-DA problem is thus stated as:

$$\min_{f \in \mathcal{F}} L_{da} = err_{D_s}^{(\rho)}(f) + d_{f,\mathcal{F}}^{(\rho)}(D_s, D_t) \quad (16)$$

In practical implementation, the multi-class margin loss may cause the gradient vanishing problem in stochastic gradient descent (SGD). As in (Zhang et al., 2019b), we choose the standard cross-entropy loss function in the source domain and adopt a modified adversarial loss function (Goodfellow et al., 2014) in the target domain. The process of minimizing L_{da} is thus decomposed into a minimax game:

$$\min_{f, \psi} L_{ent} + L_{mdd}$$
$$\max_{f'} L_{mdd} \quad (17)$$

where L_{ent} and L_{mdd} are defined as follows:

$$L_{ent} = - \sum_{x_i \in D_s} \log \sigma_{y_i}(f(\psi(x_i))) \quad (18)$$

$$L_{mdd} = \gamma \sum_{x_i \in D_s} \log[\sigma_{h_f(\psi(x_i))}(f'(\psi(x_i)))]$$
$$+ \sum_{x_i \in D_t} \log[1 - \sigma_{h_f(\psi(x_i))}(f'(\psi(x_i)))] \quad (19)$$

The notations in L_{ent} and L_{mdd} are: (1) f' is the auxiliary scoring function of f (see Figure 1). Both f and f' are used to conduct the adversarial learning, with a gradient reversed layer (GRL) (Ganin & Lempitsky, 2015) before f' to back-propagate the reversal gradient (see Figure 1). (2) σ is the softmax function, i.e., for $\mathbf{z} \in R^N$, $\sigma_j(\mathbf{z}) = e^{z_j} / \sum_{l=1}^{N} e^{z_l}$, $j = 1, ..., N$. (3) γ is the coefficient to control the trade-off between the source and target domains.

3.4. DAPNA Algorithm

The overall loss function of our DAPNA model (shown in Figure 1) is defined as follows:

$$L_{all} = L_p + \alpha(L_{ps} + L_{pt}) + \beta L_{da} \quad (20)$$

where α and β are coefficients that control the importance of the FSL loss after the feature embedding layer and the DA loss, and $\min L_{da}$ means the process of Eq. (17). We have the following theoretical analysis of our DAPNA model.

Theorem 3.2 (Learning Bound of FSL) *Let the FSL training way be N. If $D_s = D_t$ and $\widetilde{D}_s = \widetilde{D}_t$ (i.e. meta-DA degrades to the classic FSL), for any $\delta > 0$, with probability $1 - 3\delta$, the uniform learning bound for any FSL classifier f_{pt} over $\widetilde{D}_t$ is:*

$$err_{\widetilde{D}_t}(h_{f_{pt}}) \le err_{D_t}^{(\rho)}(f_{pt}) + \lambda_2 + 3\sqrt{\frac{\log \frac{2}{\delta}}{2|D_t|}}$$
$$+ \frac{2N^2}{\rho} \mathfrak{R}_{|D_t|, \widetilde{D}_t}(\Pi_1 \mathcal{F}) + \frac{2N}{\rho} \mathfrak{R}_{|D_t|, \widetilde{D}_t}(\Pi_{\mathcal{H}} \mathcal{F}) \quad (21)$$

where λ_2 is a constant independent of f_{pt}.

Theorem 3.3 (Learning Bound of DAPNA) *Let the FSL training way be N. For any $\delta > 0$, with probability $1 - 12\delta$, the uniform learning bound of DAPNA is:*

$$err_{\widetilde{D}}(h_{f_p}) + err_{\widetilde{D}_s}(h_{f_{ps}}) + err_{\widetilde{D}_t}(h_{f_{pt}}) + err_{\widetilde{D}_t}(h_f)$$
$$\le err_D^{(\rho)}(f_p) + err_{D_s}^{(\rho)}(f_{ps}) + err_{D_t}^{(\rho)}(f_{pt})$$
$$+ err_{D_s}^{(\rho)}(f) + d_{f,F}^{(\rho)}(D_s, D_t) + \lambda_3 \quad (22)$$

where λ_3 is a constant independent of f_p, f_{pt}, f_{ps}, and f.

The detailed proofs for the above two theorems can be found in the suppl. material. Note that Theorem 3 can be regarded

---

Algorithm 1 Domain Adaptation ProtoNet with Attention

Input: a large sample set $\mathcal{D}_s$, hyperparameters α, β, γ
Output: embedding functions ϕ, ψ, attention functions $\tilde{\phi}, \tilde{\psi}$
for iteration = 1,..., MaxIteration **do**
    1. Sample one $(2n)$-way k-shot episode D from $\mathcal{D}_s$ with two n-way k-shot sub-episodes D_s, D_t without class overlap, i.e., $D = D_s \bigcup D_t, D_s \bigcap D_t = \emptyset$
    2. Compute the PNA loss L_p over D with Eq. (3)
    3. Compute the PNA loss L_{ps}, L_{pt} over D_s, D_t with Eq. (6)
    4. Compute the DA loss L_{da} over D_s, D_t by running the minimax game of Eq. (17) with Eqs. (18)-(19)
    5. Compute the total loss L_{all} with Eq. (20)
    6. Update $\phi, \psi, \tilde{\phi}, \tilde{\psi}$ by Back-propagating the loss L_{all}
end for
Return $\phi, \psi, \tilde{\phi}, \tilde{\psi}$.

---

as a combination of Theorem 3.1 and Theorem 2. More importantly, we find that the overall loss L_{all} of our DAPNA model is the approximation of the upper bound on the right side of Eq. (22), if we set $\alpha = \beta = 1$ in Eq. (20). That is, we have established a theoretical guarantee for training our DAPNA model by minimizing L_{all}.

The full algorithm is outlined in Algorithm 1. In Theorem 3, we have given a theoretical analysis of our DAPNA model. To provide further supports for Theorem 3, we present illustrative results in Figure 3 (see Sec. 4.3).

4. Experiments

4.1. Datasets and Settings

Datasets (1) **miniImageNet**. This dataset is widely used for the conventional FSL setting, which consists of 100 classes selected from ILSVRC-2012 (Russakovsky et al., 2015). We follow the class split as in (Vinyals et al., 2016), with 64/16/20 classes for training/validation/test. Each class has 600 images of the size 84×84. (2) **tieredImageNet**. This benchmark (Ren et al., 2018) is also widely used for the conventional FSL setting. It is a larger subset of ILSVRC-2012, which is composed of 608 classes. Each class has about 1,300 images of the size 84×84. We use 351/97/160 classes for training/validation/test. (3) **CUB**. Under the fine-grained FSL setting, we choose the CUB-200-2011 (CUB) dataset (Wah et al., 2011), which has 200 classes and 11,788 images of birds. As in (Mangla et al., 2019), we split CUB into 100 training/50 validation/50 test classes. We resize each image to 84×84. (4) **miniImageNet → CUB**. Under the cross-domain FSL setting, we use 100 classes from miniImageNet for training, and 50/50 classes from CUB for validation/test, as in (Chen et al., 2019).

Training Episode Sampling As mentioned in Sec. 3.3, at each meta-training step, we randomly sample an episode D with two sub-episodes D_s, D_t without class overlap. Concretely, the episode D corresponds to a $(2n)$-way k-shot

q-query meta-task (with $2n * (k + q)$ images), and the sub-episode (D_s or D_t) corresponds to a n-way k-shot q-query meta-task (with $n * (k + q)$ images). Note that $D = D_s \bigcup D_t$ and $D_s \bigcap D_t = \emptyset$. In this work, we set $n = 5, k = 1/5, q = 15$ for all experiments.

Evaluation Protocols We make performance evaluation on the test set under the traditional 5-way 1-shot and 5-way 5-shot settings (15-query for each test episode), as in previous work (Vinyals et al., 2016). Concretely, we randomly sample 2,000 episodes from the test set, and then report the average accuracy (%, top-1) as well as the 95% confidence interval over all the test episodes.

Hyperparameter Selection Our DAPNA algorithm (see Algorithm 1) has only three free hyperparameters to tune: γ (see Eq. (19)) and α, β (see Eq. (20)). In this work, according to the validation performance of our DAPNA algorithm, we find the optimal hyperparameter setting $\alpha = 1, \beta = 1, \gamma = 4$ throughout all the datasets.

Backbones Three types of deep neural networks have been widely used as the backbones in previous works on FSL: Conv-4 (i.e. 4-blocks) (Vinyals et al., 2016), ResNet-12 (Mishra et al., 2018), and WRN-28-10 (Zagoruyko & Komodakis, 2016). The published results with these backbones are included in our main results (see Table 1). Note that the state-of-the-art results are typically obtained with the deepest WRN-28-10. Therefore, we only employ WRN-28-10 as our backbone, unless stated otherwise.

Implementation Details Our implementation is based on PyTorch (Paszke et al., 2017a). For optimization, we use stochastic gradient descent (SGD) with the Nesterov momentum 0.9. The initial learning rate is set to 1e-4. The implementation details between the standard and cross-domain FSL settings are different in that: (1) **Standard FSL**. We use WRN-28-10 (Zagoruyko & Komodakis, 2016) as the backbone. We resize the original 84×84 images to 80×80 and feed them to the backbone, as in (Qiao et al., 2018; Gidaris et al., 2019). We pretrain the backbone with the training set, and then train our model (initialized with the pretrained backbone) with 100 epochs, each epoch containing 100 episodes. (2) **Cross-Domain FSL**. For fair comparison with the latest work (Chen et al., 2019), we choose ResNet-18 (He et al., 2016) as backbone with the input size of 224×224. We directly train our model from scratch with 400 epochs, each epoch including 100 episodes.

4.2. Main Results

Standard FSL The comparative results under the standard FSL setting on the first three benchmark datasets are shown in Table 1. We list the backbones of different FSL methods in the second column. We have the following observations: (1) Our DAPNA model achieves new state-of-the-art perfor-

Table 1. **Comparison to the state-of-the-art on miniImageNet, tieredImageNet, and CUB**. Average 5-way few-shot classification accuracies (%) along with 95% confidence intervals are computed on the meta-test split of each dataset.

Model	Backbone	miniImageNet		tieredImageNet		CUB	
		1-shot	5-shot	1-shot	5-shot	1-shot	5-shot
(Ravi & Larochelle, 2017)	Conv-4	43.44 ± 0.77	60.60 ± 0.71	-	-	-	-
MatchingNet (Vinyals et al., 2016)	Conv-4	43.56 ± 0.84	55.31 ± 0.73	-	-	-	-
MAML (Finn et al., 2017)	Conv-4	48.70 ± 1.84	63.11 ± 0.92	51.67 ± 1.81	70.30 ± 1.75	71.29 ± 0.95	80.33 ± 0.70
ProtoNet (Snell et al., 2017)	Conv-4	49.42 ± 0.78	68.20 ± 0.66	53.31 ± 0.89	72.69 ± 0.74	71.88 ± 0.91	87.42 ± 0.48
RelationNet (Sung et al., 2018)	Conv-4	50.55 ± 0.82	65.32 ± 0.70	54.48 ± 0.93	71.32 ± 0.78	68.65 ± 0.91	81.12 ± 0.63
TPN (Liu et al., 2019)	Conv-4	55.51 ± 0.86	69.86 ± 0.65	59.91 ± 0.94	73.30 ± 0.75	-	-
(Gidaris & Komodakis, 2018)	Conv-4	56.20 ± 0.86	73.00 ± 0.64	-	-	-	-
SNAIL (Mishra et al., 2018)	ResNet-12	55.71 ± 0.99	68.88 ± 0.92	-	-	-	-
(Munkhdalai et al., 2018)	ResNet-12	56.88 ± 0.62	71.94 ± 0.57	-	-	-	-
TADAM (Oreshkin et al., 2018)	ResNet-12	58.50 ± 0.30	76.70 ± 0.30	-	-	-	-
MetaOpt (Lee et al., 2019b)	ResNet-12	62.64 ± 0.61	78.63 ± 0.46	65.99 ± 0.72	81.56 ± 0.53	80.23 ± 0.44	90.90 ± 0.23
CAN (Hou et al., 2019)	ResNet-12	63.85 ± 0.48	79.44 ± 0.34	69.89 ± 0.51	84.23 ± 0.37	-	-
PPA (Qiao et al., 2018)	WRN-28-10	59.60 ± 0.41	73.74 ± 0.19	-	-	-	-
FEAT (Ye et al., 2018)	WRN-28-10	66.69 ± 0.20	81.80 ± 0.15	-	-	-	-
LEO (Rusu et al., 2019)	WRN-28-10	61.76 ± 0.08	77.59 ± 0.12	66.33 ± 0.05	81.44 ± 0.09	68.22 ± 0.22	78.27 ± 0.16
Robust 20 (Dvornik et al., 2019)	WRN-28-10	63.46 ± 0.62	81.94 ± 0.44	-	-	-	-
(Gidaris & Komodakis, 2019)	WRN-28-10	62.96 ± 0.15	78.85 ± 0.10	68.18 ± 0.16	83.09 ± 0.12	-	-
CC+rot (Gidaris et al., 2019)	WRN-28-10	62.93 ± 0.45	79.87 ± 0.33	$\mathbf{70.53 \pm 0.51}$	84.98 ± 0.36	-	-
S2M2$_R$ (Mangla et al., 2019)	WRN-28-10	64.93 ± 0.18	83.18 ± 0.11	-	-	80.68 ± 0.81	90.85 ± 0.44
DAPNA(ours)	WRN-28-10	$\mathbf{71.88 \pm 0.22}$	$\mathbf{84.07 \pm 0.16}$	69.14 ± 0.53	$\mathbf{85.82 \pm 0.16}$	$\mathbf{82.34 \pm 0.19}$	$\mathbf{94.22 \pm 0.19}$

mance on the miniImageNet and fine-grained CUB datasets, under both 5-way 5-shot and 5-way 1-shot settings. It is worth noting that our model obtains more than 71% accuracy on miniImageNet under the 5-way 1-shot setting, outperforming the existing FSL models by a significant margin ($> 5\%$). (2) Our DAPNA model also outperforms existing FSL methods under the 5-way 5-shot setting on tieredImageNet. Although our model does not gain the highest accuracy under the 5-way 1-shot on this dataset, the gap between the best model and our DAPNA is only marginal (i.e., CC+rot – 70.53 vs. DAPNA – 69.14). (3) Overall, our DAPNA model achieves new state-of-the-art performance on the three benchmark datasets, validating the effectiveness of introducing meta-DA into meta-learning based FSL.

Cross-Domain FSL We also conduct cross-domain FSL experiments as in (Chen et al., 2019). The comparative results on miniImageNet $\rightarrow$ CUB are presented in Table 2. For alternative models, we cite the 5-way 5-shot results directly from (Chen et al., 2019), and reproduce the 5-way 1-shot results with the released code[1] of (Chen et al., 2019). It can be observed from Table 2 that: (1) Our DAPNA beats all state-of-the-art alternatives by large margins, demonstrating the effectiveness of our model under this more challenging setting. (2) The superiority of our DAPNA over all alternatives provides further evidence that the domain gap between the training and test classes under the FSL setting does exist, and introducing the DA techniques for meta-training indeed helps to alleviate the domain shift issue. (3) The improvements achieved by our DAPNA over all alternatives

[1]https://github.com/wyharveychen/CloserLookFewShot

Table 2. **Comparative results on the cross-domain miniImageNet $\rightarrow$ CUB dataset**. Average 5-way few-shot classification accuracies (%) with 95% confidence intervals are computed on the meta-test split. All models use ResNet-18 as backbone.

Model	miniImageNet $\rightarrow$ CUB	
	1-shot	5-shot
Baseline (Ravi & Larochelle, 2017)	43.34 ± 0.70	65.57 ± 0.70
Baseline++ (Chen et al., 2019)	33.04 ± 0.60	62.04 ± 0.76
MatchingNet (Vinyals et al., 2016)	45.59 ± 0.81	53.07 ± 0.74
MAML (Finn et al., 2017)	40.15 ± 0.81	51.34 ± 0.72
ProtoNet (Snell et al., 2017)	45.31 ± 0.78	62.02 ± 0.70
RelationNet (Sung et al., 2018)	42.91 ± 0.78	57.71 ± 0.73
FEAT (Ye et al., 2018)	39.00 ± 0.96	61.77 ± 0.86
DAPNA(ours)	$\mathbf{49.44 \pm 0.71}$	$\mathbf{68.33 \pm 0.68}$

under the 5-way 1-shot setting are larger than those under the 5-way 5-shot setting. This again suggests that under more challenging FSL settings, the advantages of our model become easier to recognize, thanks to its ability of explicitly addressing the domain shift problem.

4.3. Further Evaluation

Ablative Study To demonstrate the contribution of each component in our full DAPNA model, we make comparison to its simplified versions: (1) **PN**– The original ProtoNet. (2) **PNA** – Only the PNA loss L_p described in Sec. 3.2 is used. In other words, we set $\alpha = \beta = 0$ in Eq. (20) to obtain PNA. (3) **PNA+PNA*** – We just combine the PNA loss L_p over D and the PNA losses L_{ps}, L_{pt} over two sub-episodes D_s, D_t. We define the later as PNA*. This version is corresponding to the one when we set $\beta = 0$ in
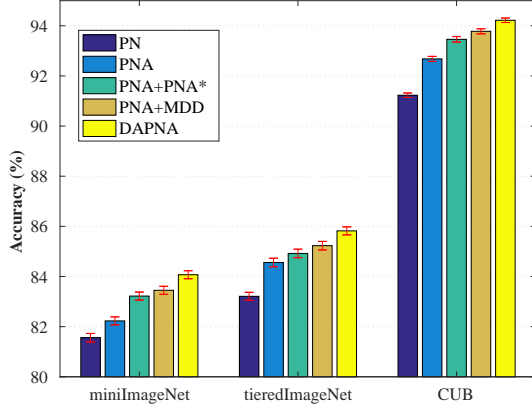
Figure 2. Ablative results for our full DAPNA model under the 5-way 5-shot settings on miniImageNet, tieredImageNet, and CUB.

(a) DAPNA   (b) PNA

Figure 3. Illustration of the changes of test MDD and test accuracy of the learned models during the training stage on miniImageNet: (a) DAPNA; (b) PNA. We randomly sample 1,000 10-way 5-shot test episodes (including 2,000 5-way 5-shot sub-episodes) to compute the test MDD and test accuracy.

Eq. (20). (4) **PNA+MDD** – our DAPNA model without using the PNA loss over two sub-episodes. That is, we set $\alpha = 0$ in Eq. (20) to obtained PNA+MDD. Note that our full DAPNA model can be denoted as PNA+MDD+PNA*. The ablative results are shown in Figure 2. It can be seen that: (i) PNA outperforms PN on all datasets, validating the effectiveness of introducing the attention mechanism into PN. (ii) The improvements achieved by PNA+PNA* over PNA show that we also need to conduct FSL optimization over two sub-episodes D_s, D_t. This is also supported by the improvements achieved by DAPNA over PNA+MDD. (iii) The superiority of PNA+MDD over PNA demonstrates the strength of introducing DA into the meta-learning based FSL framework. We can draw the same conclusion by moving on to the comparison DAPNA vs. PNA+PNA*.

Why Meta-DA Works? In the training stage, we construct each training episode with two sub-episodes without class overlap, in order to simulate the source and target domains for domain adaptation during meta-training. We claim that the introduction of DA techniques into FSL can help to enhance the model's transferability. To validate this claim, we test the learned model on the meta-test set (at each training epoch). We again construct each test episode with two sub-episodes to serve as the source and target domains to compute the MDD between them. This can be used to measure the meta-DA ability of our model. Concretely, we randomly sample 1,000 test episodes (10-way 5-shot 15-query), each of which is composed of two sub-episodes (5-way 5-shot 15-query) without class overlap. To compute the MDD (see Definition 3.1), we need two 10-way classifiers f, f' (in Eq. (19)) to classify the samples in each test episode. However, as the source and target classes are absolutely non-overlapped, the two classifiers f, f' used for recognizing the source classes could not be applied to the target classes. For simplicity, we thus select two non-parametric 10-way classifiers – Euclidean-distance and Cosine-distance based nearest neighbor classifiers. In other words, we utilize the few shots in each target class to calculate the class proto-
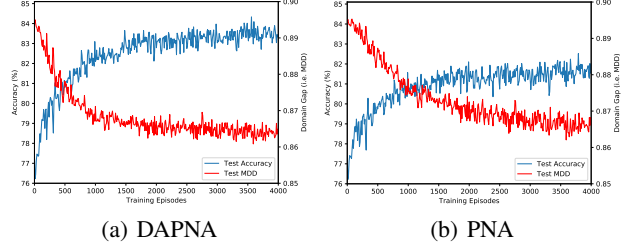
types and use nearest neighbor search methods (i.e. based either on Euclidean or on Cosine distance) to classify the rest samples in each test episode. We finally average the MDD values over 1,000 test episodes.

In this work, to explain why meta-DA works, we conduct a group of experiments on the three FSL benchmark datasets: the obtained results on miniImageNet are shown in Figure 3, while the similar results on TieredImageNet and CUB are provided in the suppl. material. We can draw the following conclusions: (1) For our DAPNA model, the lower the test MDD is, the higher the test accuracy is. This observation coincides with our theoretical analysis in Theorem 3: When the MDD loss is explicitly reduced by meta-DA during meta-training, the meta-DA ability of our DAPNA model is enforced; In the test stage, this meta-DA ability still holds and the test MDD tends to take a lower value, thus leading to higher test accuracy. (2) As the number of training epochs increases, both PNA and DAPNA obtain higher test accuracies. However, our DAPNA converges much faster than PNA, showing that explicitly introducing meta-DA into meta-learning based FSL can speed up the convergence of the episodic training process. (3) The reduction of the MDD loss on the meta-test set owes to the exploration of the relations across different meta-tasks (i.e. sub-episodes) during meta-training. This suggests that modeling meta-task relations is crucial for meta-learning based FSL.

5. Conclusions

In this paper, we for the first time identify the domain shift problem caused by the class difference in the source and target data as a main challenge in FSL. Based on this understanding, we propose to tackle the DA problem explicitly in FSL in a episodic training manner. We further provide theoretical analysis of the learning bound for our proposed algorithm. The state-of-the-art performance demonstrates the superiority of our algorithm, and also validates our claim that the class-difference caused domain shift issue in FSL must be explicitly addressed. It is worth noting that our meta-DA strategy can be easily deployed in any existing

episodic-training based FSL model.

References

Ben-David, S., Blitzer, J., Crammer, K., Kulesza, A., Pereira, F., and Vaughan, J. W. A theory of learning from different domains. *Machine Learning*, 79(1-2):151–175, 2010.

Chen, W., Liu, Y., Kira, Z., Wang, Y. F., and Huang, J. A closer look at few-shot classification. In *ICLR*, 2019.

Dvornik, N., Schmid, C., and Mairal, J. Diversity with co-operation: Ensemble methods for few-shot classification. In *ICCV*, 2019.

Finn, C., Abbeel, P., and Levine, S. Model-agnostic meta-learning for fast adaptation of deep networks. In *ICML*, pp. 1126–1135, 2017.

Finn, C., Xu, K., and Levine, S. Probabilistic model-agnostic meta-learning. In *NeurIPS*, pp. 9537–9548, 2018.

Ganin, Y. and Lempitsky, V. S. Unsupervised domain adaptation by backpropagation. In *ICML*, pp. 1180–1189, 2015.

Ganin, Y., Ustinova, E., Ajakan, H., Germain, P., Larochelle, H., Laviolette, F., Marchand, M., and Lempitsky, V. S. Domain-adversarial training of neural networks. *Journal of Machine Learning Research (JMLR)*, 17:59:1–59:35, 2016.

Gidaris, S. and Komodakis, N. Dynamic few-shot visual learning without forgetting. In *CVPR*, pp. 4367–4375, 2018.

Gidaris, S. and Komodakis, N. Generating classification weights with GNN denoising autoencoders for few-shot learning. In *CVPR*, pp. 21–30, 2019.

Gidaris, S., Bursuc, A., Komodakis, N., Perez, P., and Cord, M. Boosting few-shot visual learning with self-supervision. In *ICCV*, 2019.

Goodfellow, I. J., Pouget-Abadie, J., Mirza, M., Xu, B., Warde-Farley, D., Ozair, S., Courville, A. C., and Bengio, Y. Generative adversarial nets. In *NeurIPS*, pp. 2672–2680, 2014.

Gretton, A., Smola, A., Huang, J., Schmittfull, M., Borgwardt, K., and Schölkopf, B. *Covariate shift and local learning by distribution matching*, pp. 131–160. MIT Press, 2009.

He, K., Zhang, X., Ren, S., and Sun, J. Deep residual learning for image recognition. In *CVPR*, pp. 770–778, 2016.

Hou, R., Chang, H., MA, B., Shan, S., and Chen, X. Cross attention network for few-shot classification. In *NeurIPS*, pp. 4005–4016, 2019.

Kim, J., Kim, T., Kim, S., and Yoo, C. D. Edge-labeling graph neural network for few-shot learning. In *CVPR*, pp. 11–20, 2019.

Lee, J., Lee, Y., Kim, J., Kosiorek, A. R., Choi, S., and Teh, Y. W. Set transformer: A framework for attention-based permutation-invariant neural networks. In *ICML*, 2019a.

Lee, K., Maji, S., Ravichandran, A., and Soatto, S. Meta-learning with differentiable convex optimization. In *CVPR*, pp. 10657–10665, 2019b.

Lee, Y. and Choi, S. Gradient-based meta-learning with learned layerwise metric and subspace. In *ICML*, pp. 2933–2942, 2018.

Li, A., Luo, T., Xiang, T., Huang, W., and Wang, L. Few-shot learning with global class representations. In *ICCV*, 2019.

Li, F., Fergus, R., and Perona, P. One-shot learning of object categories. *IEEE Transactions on Pattern Analysis and Machine Intelligence (TPAMI)*, 28(4):594–611, 2006.

Li, Z., Zhou, F., Chen, F., and Li, H. Meta-sgd: Learning to learn quickly for few shot learning. *CoRR*, abs/1707.09835, 2017.

Liu, Y., Lee, J., Park, M., Kim, S., Yang, E., Hwang, S. J., and Yang, Y. Learning to propagate labels: Transductive propagation network for few-shot learning. In *ICLR*, 2019.

Long, M., Cao, Y., Wang, J., and Jordan, M. I. Learning transferable features with deep adaptation networks. In *ICML*, pp. 97–105, 2015.

Long, M., Cao, Z., Wang, J., and Jordan, M. I. Conditional adversarial domain adaptation. In *NeurIPS*, pp. 1647–1657, 2018.

Mangla, P., Singh, M., Sinha, A., Kumari, N., Balasubramanian, V. N., and Krishnamurthy, B. Charting the right manifold: Manifold mixup for few-shot learning. *CoRR*, abs/1907.12087, 2019.

Mansour, Y., Mohri, M., and Rostamizadeh, A. Domain adaptation: Learning bounds and algorithms. In *COLT*, 2009.

McCann, B., Bradbury, J., Xiong, C., and Socher, R. Learned in translation: Contextualized word vectors. In *NeurIPS*, pp. 6297–6308, 2017.

Mishra, N., Rohaninejad, M., Chen, X., and Abbeel, P. A simple neural attentive meta-learner. In *ICLR*, 2018.

Mohri, M., Rostamizadeh, A., and Talwalkar, A. *Foundations of Machine Learning*. Adaptive computation and machine learning. MIT Press, 2012.

Motiian, S., Jones, Q., Iranmanesh, S. M., and Doretto, G. Few-shot adversarial domain adaptation. In *NeurIPS*, 2017.

Muandet, K., Balduzzi, D., and Schölkopf, B. Domain generalization via invariant feature representation. In *ICML*, pp. 10–18, 2013.

Munkhdalai, T. and Yu, H. Meta networks. In *ICML*, pp. 2554–2563, 2017.

Munkhdalai, T., Yuan, X., Mehri, S., and Trischler, A. Rapid adaptation with conditionally shifted neurons. In *ICML*, pp. 3661–3670, 2018.

Oreshkin, B. N., López, P. R., and Lacoste, A. TADAM: task dependent adaptive metric for improved few-shot learning. In *NeurIPS*, pp. 719–729, 2018.

Pan, S. J. and Yang, Q. A survey on transfer learning. *IEEE Transactions on Knowledge and Data Engineering (TKDE)*, 22(10):1345–1359, 2010.

Paszke, A., Gross, S., Chintala, S., Chanan, G., Yang, E., Devito, Z., Lin, Z., Desmaison, A., Antiga, L., and Lerer, A. Automatic differentiation in pytorch. In *NeurIPS, Workshop*, 2017a.

Paszke, A., Gross, S., Chintala, S., Chanan, G., Yang, E., DeVito, Z., Lin, Z., Desmaison, A., Antiga, L., and Lerer, A. Automatic differentiation in pytorch. In *NeurIPS, Workshop*, 2017b.

Qiao, S., Liu, C., Shen, W., and Yuille, A. L. Few-shot image recognition by predicting parameters from activations. In *CVPR*, pp. 7229–7238, 2018.

Ranzato, M., Boureau, Y., Chopra, S., and LeCun, Y. A unified energy-based framework for unsupervised learning. In *AISTATS*, pp. 371–379, 2007.

Ravi, S. and Larochelle, H. Optimization as a model for few-shot learning. In *ICLR*, 2017.

Ren, M., Triantafillou, E., Ravi, S., Snell, J., Swersky, K., Tenenbaum, J. B., Larochelle, H., and Zemel, R. S. Meta-learning for semi-supervised few-shot classification. In *ICLR*, 2018.

Ren, M., Liao, R., Fetaya, E., and Zemel, R. Incremental few-shot learning with attention attractor networks. In *NeurIPS*, pp. 5276–5286, 2019.

Russakovsky, O., Deng, J., Su, H., Krause, J., Satheesh, S., Ma, S., Huang, Z., Karpathy, A., Khosla, A., Bernstein, M., Berg, A. C., and Fei-Fei, L. ImageNet large scale visual recognition challenge. *International Journal of Computer Vision (IJCV)*, 115(3):211–252, 2015.

Rusu, A. A., Rao, D., Sygnowski, J., Vinyals, O., Pascanu, R., Osindero, S., and Hadsell, R. Meta-learning with latent embedding optimization. In *ICLR*, 2019.

Snell, J., Swersky, K., and Zemel, R. Prototypical networks for few-shot learning. In *NeurIPS*, pp. 4077–4087, 2017.

Sohn, K., Shang, W., Yu, X., and Chandraker, M. Unsupervised domain adaptation for distance metric learning. In *ICLR*, 2019.

Sun, Q., Liu, Y., Chua, T., and Schiele, B. Meta-transfer learning for few-shot learning. In *CVPR*, pp. 403–412, 2019.

Sung, F., Yang, Y., Zhang, L., Xiang, T., Torr, P. H. S., and Hospedales, T. M. Learning to compare: Relation network for few-shot learning. In *CVPR*, pp. 1199–1208, 2018.

Tseng, H.-Y., Lee, H.-Y., Huang, J.-B., and Yang, M.-H. Cross-domain few-shot classification via learned feature-wise transformation. In *ICLR*, 2020.

Valiant, L. G. A theory of the learnable. *Commun. ACM*, 27 (11):1134–1142, 1984.

Vinyals, O., Blundell, C., Lillicrap, T., Kavukcuoglu, K., and Wierstra, D. Matching networks for one shot learning. In *NeurIPS*, pp. 3630–3638, 2016.

Wah, C., Branson, S., Welinder, P., Perona, P., and Belongie, S. The caltech-ucsd birds-200-2011 dataset. Technical Report CNS-TR-2011-001, California Institute of Technology, 2011.

Xing, C., Rostamzadeh, N., Oreshkin, B., and O. Pinheiro, P. O. Adaptive cross-modal few-shot learning. In *NeurIPS*, pp. 4848–4858, 2019.

Ye, H., Hu, H., Zhan, D., and Sha, F. Learning embedding adaptation for few-shot learning. *CoRR*, abs/1812.03664, 2018.

Zagoruyko, S. and Komodakis, N. Wide residual networks. In *BMVC*, 2016.

Zhang, J., Zhao, C., Ni, B., Xu, M., and Yang, X. Variational few-shot learning. In *ICCV*, 2019a.

Zhang, Y., Liu, T., Long, M., and Jordan, M. I. Bridging theory and algorithm for domain adaptation. In *ICML*, pp. 7404–7413, 2019b.

APPENDIX

In this material, we provide more details and explanations for our proposed DAPNA model. We give the proofs of our theoretical results in Section 6, describe our computing infrastructure in Section 7, introduce the specific structure of our feature embedding layer in Section 8, explain more implementation details in our experiments in Section 9, and give insightful illustration results to show why Meta-DA strategy works in Section 10.

6. Proofs of Theoretical Results

Theorem 3.1 (Learning Bound of DA) *For any* $\delta > 0$, *with probability* $1 - 3\delta$, *the uniform learning bound for any classifier f over $\widetilde{D}_t$ is given by:*

$$
\begin{aligned}
err_{\widetilde{D}_t}(h_f) &\leq err_{D_s}^{(\rho)}(f) + d_{f,F}^{(\rho)}(D_s, D_t) + \lambda_1 \\
&+ \frac{2N^2}{\rho}\mathfrak{R}_{|D_s|,\widetilde{D}_s}(\Pi_1\mathcal{F}) + \frac{N}{\rho}\mathfrak{R}_{|D_s|,\widetilde{D}_s}(\Pi_\mathcal{H}\mathcal{F}) \\
&+ \frac{N}{\rho}\mathfrak{R}_{|D_t|,\widetilde{D}_t}(\Pi_\mathcal{H}\mathcal{F}) + 2\sqrt{\frac{\log\frac{2}{\delta}}{2|D_s|}} + \sqrt{\frac{\log\frac{2}{\delta}}{2|D_t|}}
\end{aligned} \tag{23}
$$

where λ_1 is a constant independent of f, $\mathfrak{R}_{|D|,\widetilde{D}}(\mathcal{F})$ is the Rademacher Complexity of $\mathcal{F}$ w.r.t. the sample set D drawn from distribution $\widetilde{D}$, $\Pi_\mathcal{H}(\mathcal{F}) \triangleq \{x \mapsto f(x,h(x))|h \in \mathcal{H}, f \in \mathcal{F}\}, \Pi_1\mathcal{F} \triangleq \{x \mapsto f(x,y)|y \in \mathcal{Y}, f \in \mathcal{F}\}$, and N is the number of classes in $\mathcal{C}_s$ (i.e. $N = |\mathcal{C}_s|$).

As we have mentioned in the main paper, by regarding sub-episodes as domains, the above theorem can be easily proven just as Theorem 3.7 of (Zhang et al., 2019b), which is ignored for compactness.

Theorem 3.2 (Learning Bound of FSL) *Let the FSL training way be N. If $D_s = D_t$ and $\widetilde{D}_s = \widetilde{D}_t$ (i.e. meta-DA degrades to the classic FSL), for any $\delta > 0$, with probability $1 - 3\delta$, the uniform learning bound for any FSL classifier f_{pt} over $\widetilde{D}_t$ is:*

$$
\begin{aligned}
err_{\widetilde{D}_t}(h_{f_{pt}}) &\leq err_{D_t}^{(\rho)}(f_{pt}) + \lambda_2 + 3\sqrt{\frac{\log\frac{2}{\delta}}{2|D_t|}} \\
&+ \frac{2N^2}{\rho}\mathfrak{R}_{|D_t|,\widetilde{D}_t}(\Pi_1\mathcal{F}) + \frac{2N}{\rho}\mathfrak{R}_{|D_t|,\widetilde{D}_t}(\Pi_\mathcal{H}\mathcal{F})
\end{aligned} \tag{24}
$$

where λ_2 is a constant independent of classifier f_{pt}.

Proof. Since $D_s = D_t, \widetilde{D}_s = \widetilde{D}_t$, then,

$$
\begin{aligned}
&d_{f,F}^{(\rho)}(D_s, D_t) \\
&= \sup_{f' \in \mathcal{F}} (\text{disp}_{D_t}^{(\rho)}(f', f) - \text{disp}_{D_s}^{(\rho)}(f', f)) \\
&= \sup_{f' \in \mathcal{F}} (\text{disp}_{D_t}^{(\rho)}(f', f) - \text{disp}_{D_t}^{(\rho)}(f', f)) = 0
\end{aligned}
$$

From Theorem 3.1, for any FSL classifier f_{pt} over $\widetilde{D}_t$,

$$
\begin{aligned}
err_{\widetilde{D}_t}(h_{f_{pt}}) &\leq err_{D_t}^{(\rho)}(f_{pt}) + \lambda_2 + 3\sqrt{\frac{\log\frac{2}{\delta}}{2|D_t|}} \\
&+ \frac{2N^2}{\rho}\mathfrak{R}_{|D_t|,\widetilde{D}_t}(\Pi_1\mathcal{F}) + \frac{2N}{\rho}\mathfrak{R}_{|D_t|,\widetilde{D}_t}(\Pi_\mathcal{H}\mathcal{F})
\end{aligned}
$$

where $\lambda_2 = \lambda(\rho, \mathcal{F}, \widetilde{D}_t)$ is independent of classifier f_{pt}. ∎

Corollary 6.1 *Let the FSL training way be $n(< N)$. For any $\delta > 0$, with probability $1 - 3\delta$, the uniform learning bound for any FSL classifier f_{pt} over $\widetilde{D}_t^{(n)}$ is:*

$$
\begin{aligned}
err_{\widetilde{D}_t^{(n)}}(h_{f_{pt}}) &\leq err_{D_t^{(n)}}^{(\rho)}(f_{pt}) + \lambda_2^{(n)} + 3\sqrt{\frac{\log\frac{2}{\delta}}{2|D_t^{(n)}|}} \\
&+ \frac{2n^2}{\rho}\mathfrak{R}_{|D_t^{(n)}|,\widetilde{D}_t^{(n)}}(\Pi_1\mathcal{F}_n) + \frac{2n}{\rho}\mathfrak{R}_{|D_t^{(n)}|,\widetilde{D}_t^{(n)}}(\Pi_{\mathcal{H}_n}\mathcal{F}_n)
\end{aligned} \tag{25}
$$

where $D_t^{(n)} \sim \widetilde{D}_t^{(n)}$, $\widetilde{D}_t^{(n)}$ is the distribution of n-way episodes. $\mathcal{H}_n \triangleq \{h : x \to y|y \in \{1, 2, ..., n\}\}, \mathcal{F}_n$ is the hypothesis space of n-way scoring functions. $\Pi_{\mathcal{H}_n}(\mathcal{F}_n) \triangleq \{x \mapsto f(x, h(x))|h \in \mathcal{H}_n, f \in \mathcal{F}_n\}, \Pi_1\mathcal{F}_n \triangleq \{x \mapsto f(x,y)|y \in \{1, 2, ..., n\}, f \in \mathcal{F}_n\}. \lambda_2^{(n)} = \lambda(\rho, \mathcal{F}_n, \widetilde{D}_t^{(n)})$ is a constant independent of f_{pt}.

Note that Corollary 6.1 gives the learning bound for any n-way FSL classifier over n-way episode distribution $\widetilde{D}_t^{(n)}$. For clarity and notation consistency, we still assume the FSL training way is N, and we can obtain the overall learning bound of DAPNA by combining Theorem 3.1 and 3.2.

Theorem 3.3 (Learning Bound of DAPNA) *Let the FSL training way be N. For any $\delta > 0$, with probability $1 - 12\delta$, the uniform learning bound of DAPNA is:*

$$
\begin{aligned}
&err_{\widetilde{D}}(h_{f_p}) + err_{\widetilde{D}_s}(h_{f_{ps}}) + err_{\widetilde{D}_t}(h_{f_{pt}}) + err_{\widetilde{D}_t}(h_f) \\
&\leq err_D^{(\rho)}(f_p) + err_{D_s}^{(\rho)}(f_{ps}) + err_{D_t}^{(\rho)}(f_{pt}) \\
&+ err_{D_s}^{(\rho)}(f) + d_{f,F}^{(\rho)}(D_s, D_t) + \lambda_3
\end{aligned}
$$

where f_p, f_{ps}, f_{pt} are FSL classifiers over $\widetilde{D}, \widetilde{D}_s, \widetilde{D}_t$ respectively, f is the classifier used in DA, and λ_3 is a constant.

Proof. From Theorem 3.2, for the FSL classifier f_p, f_{ps} over $\widetilde{D}, \widetilde{D}_s$ respectively, we have for any $\delta > 0$, with probability $1 - 3\delta$,

$$
\begin{aligned}
err_{\widetilde{D}}(h_{f_p}) &\leq err_D^{(\rho)}(f_p) + \lambda_4 + 3\sqrt{\frac{\log\frac{2}{\delta}}{2|D|}} \\
&+ \frac{2N^2}{\rho}\mathfrak{R}_{|D|,\widetilde{D}}(\Pi_1\mathcal{F}) + \frac{2N}{\rho}\mathfrak{R}_{|D|,\widetilde{D}}(\Pi_\mathcal{H}\mathcal{F})
\end{aligned} \tag{26}
$$

Table 3. **The ablative results of whether use feature embedding layer (FEL) within DAPNA on miniImageNet, tieredImageNet, and CUB**. Average 5-way 5-shot classification accuracies (%) along with 95% confidence intervals are computed on the meta-test split of each dataset.

With FEL?	miniImageNet	tieredImageNet	CUB
W/O	83.51 ± 0.15	85.87 ± 0.15	94.20 ± 0.19
W	$\mathbf{84.07 \pm 0.16}$	$\mathbf{85.96 \pm 0.16}$	$\mathbf{94.22 \pm 0.19}$

Table 4. **The comparison results of different training strategies under the 5-way 5-shot test setting on three FSL datasets**. The 'n-way-5-shot' training strategy means that during the training stage one episode D contains n classes and 5 shot per class.

Training Strategy	miniImageNet	tieredImageNet	CUB
10-way-5-shot	$\mathbf{84.07 \pm 0.16}$	85.82 ± 0.15	$\mathbf{94.22 \pm 0.19}$
20-way-5-shot	83.96 ± 0.18	$\mathbf{85.96 \pm 0.16}$	93.61 ± 0.19
30-way-5-shot	83.22 ± 0.16	84.62 ± 0.17	93.16 ± 0.09

$$err_{\widetilde{D}_s}(h_{f_{ps}}) \leq err_{D_s}^{(\rho)}(f_{ps}) + \lambda_5 + 3\sqrt{\frac{\log\frac{2}{\delta}}{2|D_s|}}$$
$$+ \frac{2N^2}{\rho}\mathfrak{R}_{|D_s|,\widetilde{D}_s}(\Pi_1\mathcal{F}) + \frac{2N}{\rho}\mathfrak{R}_{|D_s|,\widetilde{D}_s}(\Pi_{\mathcal{H}}\mathcal{F}) \quad (27)$$

where constants $\lambda_4 = \lambda(\rho, \mathcal{F}, \widetilde{D})$, $\lambda_5 = \lambda(\rho, \mathcal{F}, \widetilde{D}_s)$ are independent of f_p, f_{ps} respectively. Combining Eq. (23)-(27), we can obtain:

$$err_{\widetilde{D}}(h_{f_p}) + err_{\widetilde{D}_s}(h_{f_{ps}}) + err_{\widetilde{D}_t}(h_{f_{pt}}) + err_{\widetilde{D}_t}(h_f)$$
$$\leq err_D^{(\rho)}(f_p) + err_{D_s}^{(\rho)}(f_{ps}) + err_{D_t}^{(\rho)}(f_{pt})$$
$$+ err_{D_s}^{(\rho)}(f) + d_{f,F}^{(\rho)}(D_s, D_t) + \lambda_3$$

where λ_3 is a constant independent of f_p, f_{pt}, f_{ps}, and f:

$$\lambda_3 = \frac{2N^2}{\rho}\mathfrak{R}_{|D|,\widetilde{D}}(\Pi_1\mathcal{F}) + \frac{2N}{\rho}\mathfrak{R}_{|D|,\widetilde{D}}(\Pi_{\mathcal{H}}\mathcal{F})$$
$$+ \frac{4N^2}{\rho}\mathfrak{R}_{|D_s|,\widetilde{D}_s}(\Pi_1\mathcal{F}) + \frac{3N}{\rho}\mathfrak{R}_{|D_s|,\widetilde{D}_s}(\Pi_{\mathcal{H}}\mathcal{F})$$
$$+ \frac{2N^2}{\rho}\mathfrak{R}_{|D_t|,\widetilde{D}_t}(\Pi_1\mathcal{F}) + \frac{3N}{\rho}\mathfrak{R}_{|D_t|,\widetilde{D}_t}(\Pi_{\mathcal{H}}\mathcal{F})$$
$$+ \sum_{l=1,l\neq 3}^{5}\lambda_l + 3\sqrt{\frac{\log\frac{2}{\delta}}{2|D|}} + 5\sqrt{\frac{\log\frac{2}{\delta}}{2|D_s|}} + 4\sqrt{\frac{\log\frac{2}{\delta}}{2|D_t|}}$$

∎

7. Computing Infrastructure

We conduct our DAPNA algorithm based on PyTorch (Paszke et al., 2017b) framework. We run all deep learning experiments on a platform with 4 NVIDIA GeForce GTX TITAN V GPUs, each containing 12G memory.

8. Ablation Study for Feature Embedding Layer (FEL)

(Sohn et al., 2019) proposes a *Feature Transfer Network* to transform the instance features to be domain confused while still maintaining the features from the same domain discriminative. Inspired by this, we add an encoder-decoder network on the top of the base backbone to transform the

(a) DAPNA_tieredImageNet   (b) PNA_tieredImageNet
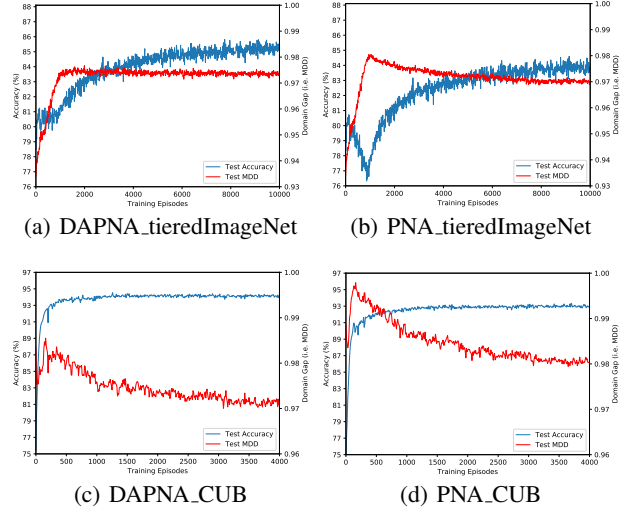
(c) DAPNA_CUB   (d) PNA_CUB

Figure 4. Illustration of the changes of test accuracy and test MDD during the training stage under the 5-way 5-shot setting on tiered-ImageNet and CUB. We randomly sample 2,000 test episodes (including 1,000 source-target episodes) to compute the test accuracy and test MDD.

original image visual features to be more domain confused. For simplicity, we use two linear layers as the encoder-decoder network. The first linear layer can be considered as a dimension reduction structure, which reduces the feature dimension to the half. Then the second linear layer will ascend the dimension of the dimension-reduced feature to that of the original features. The role of our encoder-decoder network is similar to the original Auto-encoder in (Ranzato et al., 2007). Our experiment results in Table 3 validate the effectiveness of the simple encoder-decoder network.

9. Influence of Meta-Training Way

In our experiments, we find that different training way strategies obtain different performance on different datasets. We present the detailed results in Table 4. As episode splitting strategy is our major novelty, we provide concrete experiment results under different training way environments.
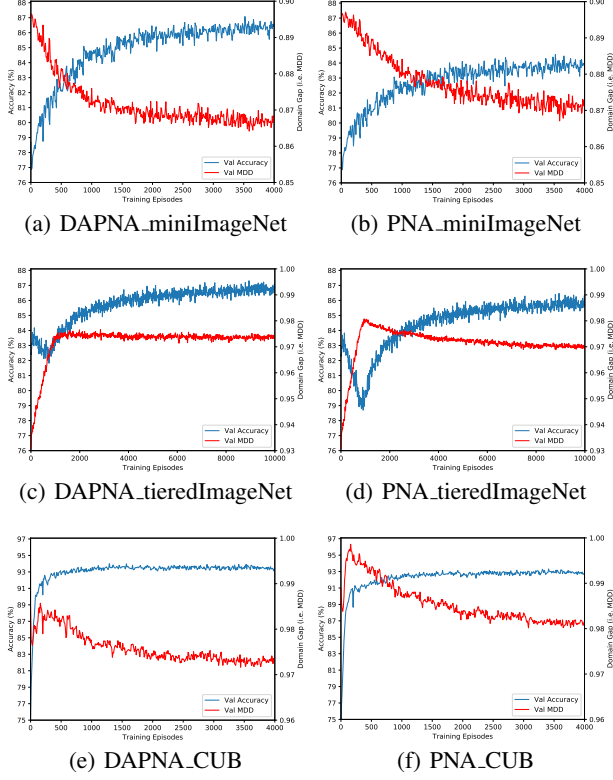
(a) DAPNA_miniImageNet

(b) PNA_miniImageNet

(c) DAPNA_tieredImageNet

(d) PNA_tieredImageNet

(e) DAPNA_CUB

(f) PNA_CUB

Figure 5. Illustration of the changes of val accuracy and val MDD during the training stage under the 5-way 5-shot setting on mini-ImageNet, tieredImageNet and CUB. We randomly sample 2,000 test episodes to compute the val accuracy and val MDD.

10. Why Meta-DA Works?

In Figure 4, We present the illustration of the changes of test accuracy and test MDD during the training stage under the 5-way 5-shot setting on tieredImageNet and CUB. As mentioned in the main paper, We randomly sample 2,000 test episodes (including 1,000 source-target episodes) to compute the test accuracy and test MDD. The performance of our DAPNA model on these two datasets is similar to that on miniImageNet in the main paper, which validates the merits of introducing the DA module into FSL optimization framework. Moreover, we conduct similar experiments over validation set on these three FSL datasets, the performance (see Figure 5) is analogous to that in test set.